Radiofrequency Heating and AI

Alvaro Sanchez-Villar

June 11, 2025

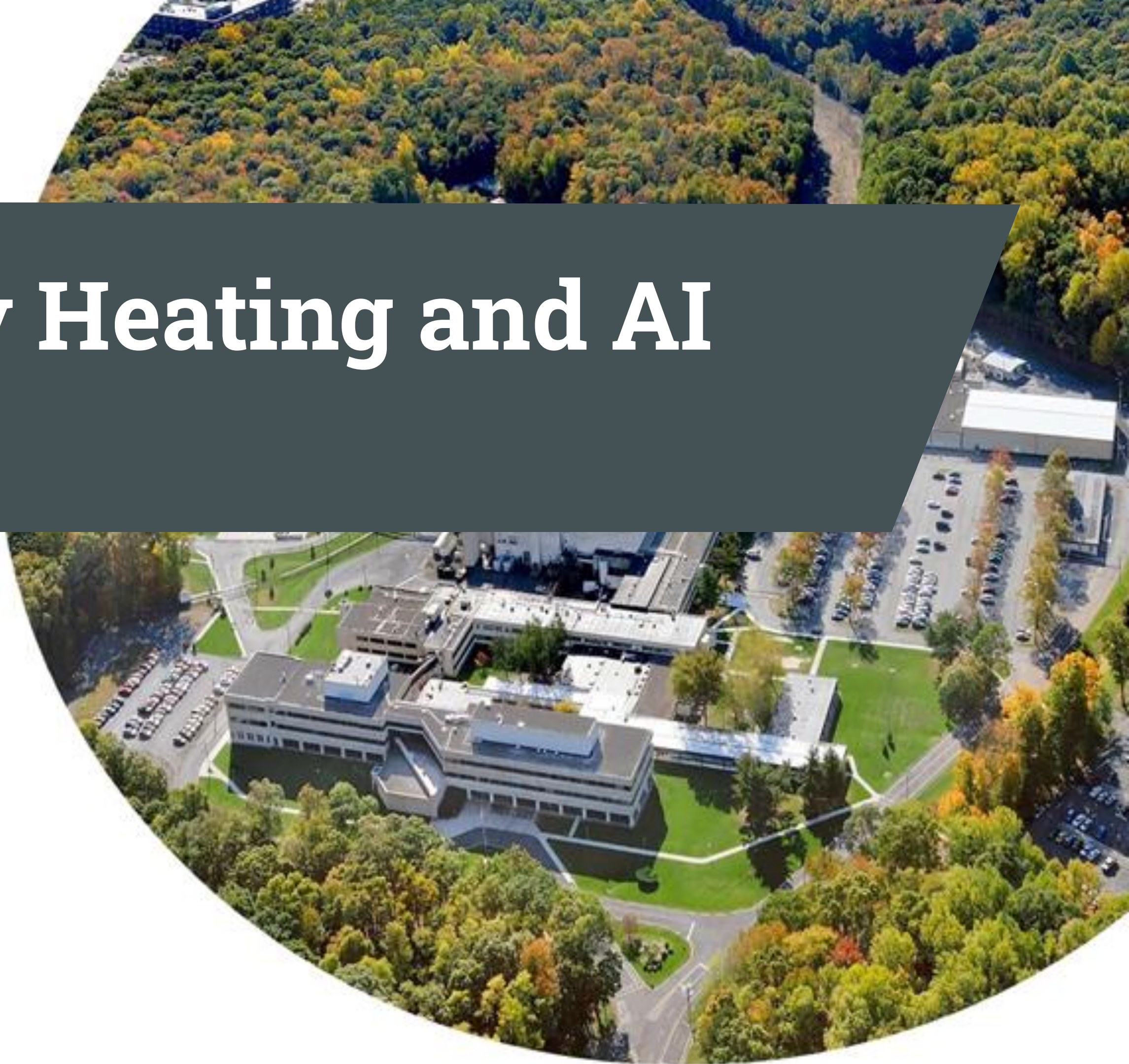

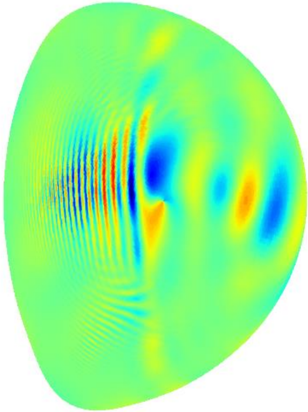

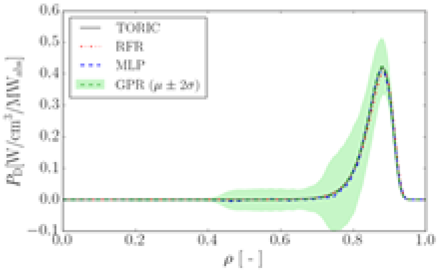

A bit about me and how I got here!

- B.S. Aerospace Engineering
- M.S. Aeronautical Engineering

uc3m | Universidad Carlos III de Madrid

TU Delft

- Ph.D. Fluid Mechanics (Plasma Physics)
- Visiting Researcher at ONERA (France)

ONERA THE FRENCH AEROSPACE LAB

- On a personal note, I enjoy painting, cooking and basketball

My role at PPPL

- Associate Research Physicist
- Computational Sciences Department

- Research interests:
  - Artificial intelligence and Machine learning
  - Radio-frequency actuator modeling

RF waves propagate in the ionosphere and magnetosphere

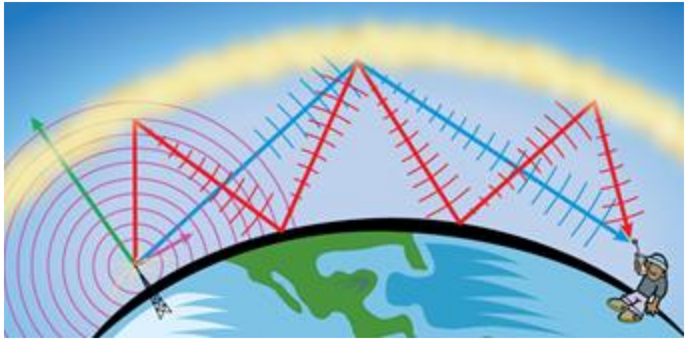

Source: NOAA

The propagation of radio waves relies in the reflection/transmission characteristics of the ionospheric plasma

Waves in the magnetosphere carry and couple energy, causing significant charged particle losses in Earth's atmosphere

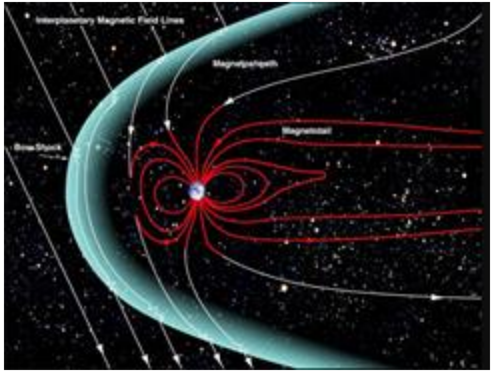

Source: NASA

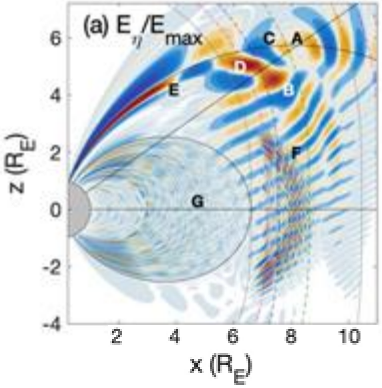

Source: Kim et al. GRL (2023)

RF waves also in solar corona

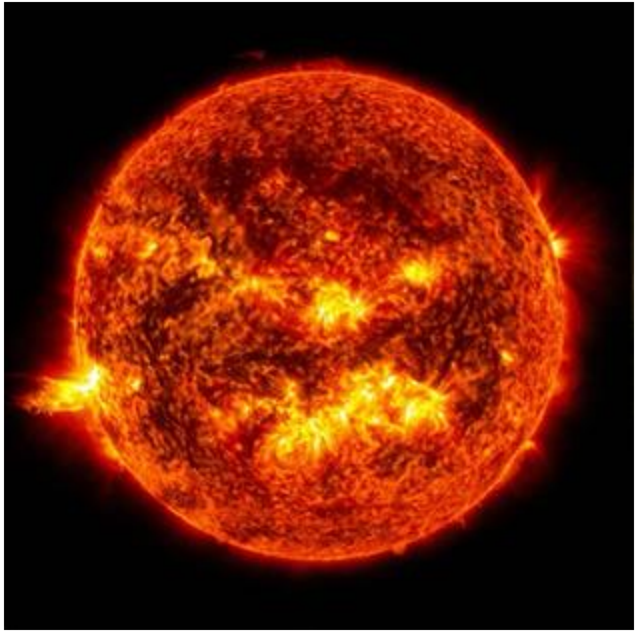

Source: NASA

Studies suggest that Alfvén wave propagation and reflection in the solar corona drive turbulence and help heat the solar corona

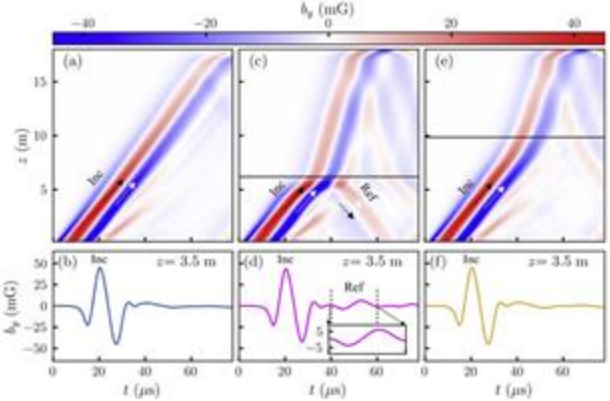

Source: Bose et al. The Astrophysical Journal (2024)

Also in space plasma thrusters!

Electrodeless Plasma Thrusters

RF HEATING SOURCE + MAGNETIC NOZZLE (MN) = PROPULSION

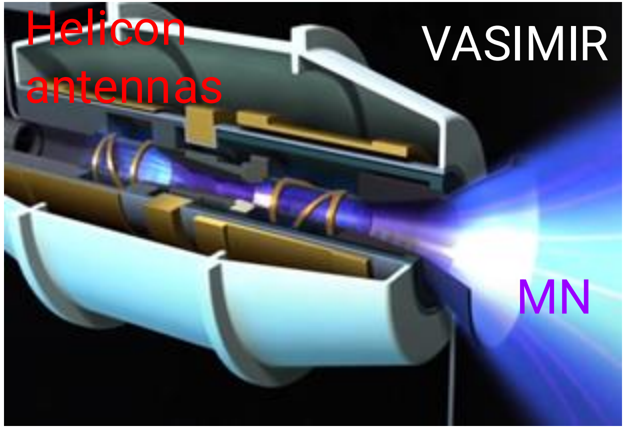

RF waves also exist in fusion devices: what is their role?

Emission/Instabilities Diagnostics:

1. Microwave reflectometers
2. Electron Cyclotron Emisison
3. Thomson scattering
4. Soft X-rays diodes/cameras
5. Etc…

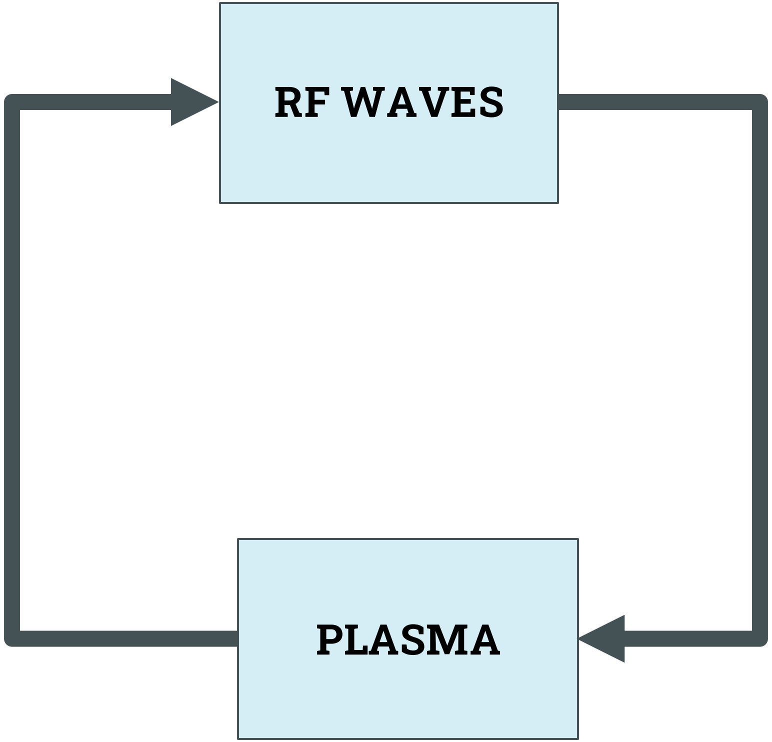

Transfer momentum and energy to plasmas Applications:

1. **Bulk heating**
2. Non-inductive current drive
1. Fast control of profiles, scenario & impurity
2. Wall conditioning
3. MHD-Instability suppression
4. Fast-ion tailoring
5. Start-up & breakdown
6. Etc…

The key frequencies in fusion devices

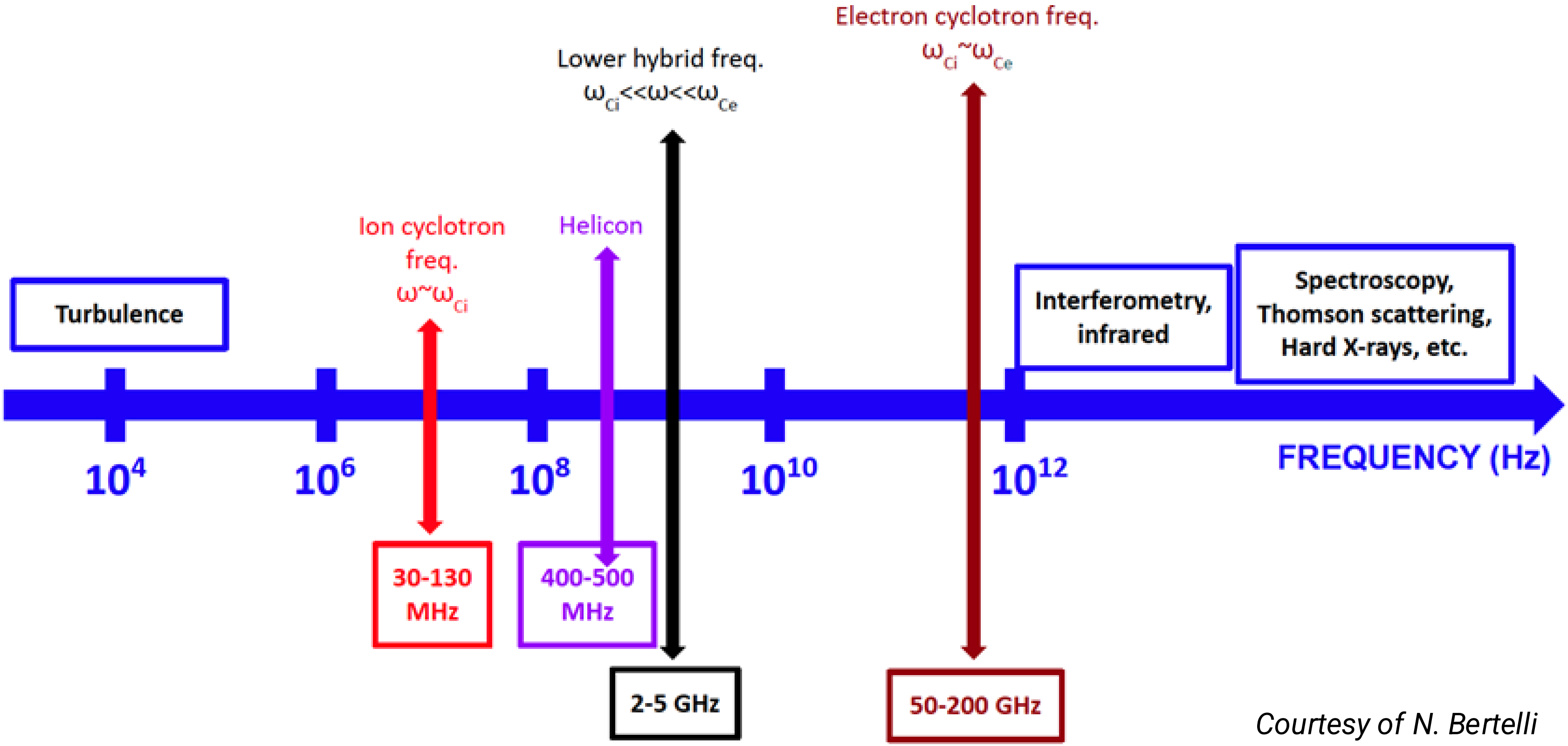

Courtesy of N. Bertelli

The RF modeling approaches are scenario dependent

- Maxwell's Equations + Plasma model

$$\nabla \times \boldsymbol{E} = -\frac{1}{c}\frac{\partial \boldsymbol{B}}{\partial t}, \qquad \nabla \times \boldsymbol{B} = \frac{4\pi}{c}\boldsymbol{J} + \frac{1}{c}\frac{\partial \boldsymbol{E}}{\partial t}.$$

- Fluid models (e.g. cold plasma approximation)
  - Local / simplified dispersion relation
  - wave propagation and absorption can be explained by the CMA diagram

$$S(\omega) = 1 - \sum_s \frac{\omega_{ps}^2}{\omega(\omega + i\nu_s) - \omega_{cs}^2}, \qquad D(\omega) = \sum_s \frac{\omega_{ps}^2\,\omega_{cs}}{\omega(\omega + i\nu_s) - \omega_{cs}^2}, \qquad P(\omega) = 1 - \sum_s \frac{\omega_{ps}^2}{\omega(\omega + i\nu_s)}.$$

$$\varepsilon_{\text{cold}}(\omega) = \begin{pmatrix} S & -i\,D & 0 \\ i\,D & S & 0 \\ 0 & 0 & P \end{pmatrix}, \quad \mathbf{b} \parallel \hat{z},\ \mathbf{k} \text{ in } x\!-\!z$$

$$\omega_{cs} \equiv \frac{q_s B_0}{m_s}, \qquad \omega_{ps} \equiv \sqrt{\frac{4\pi q_s^2 n_s}{m_s}},$$

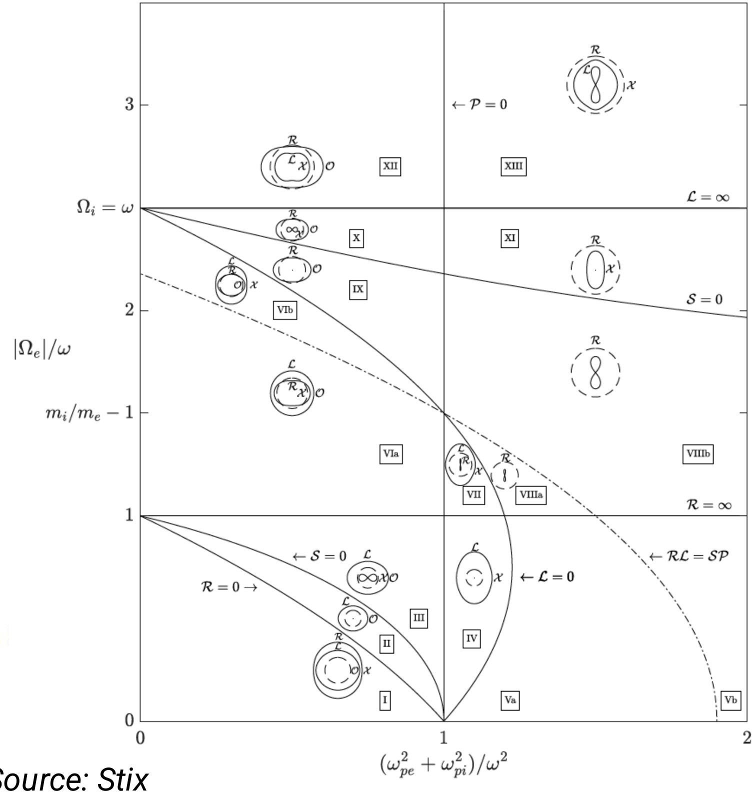

Source: Stix

A scenario where the cold plasma model may suffice

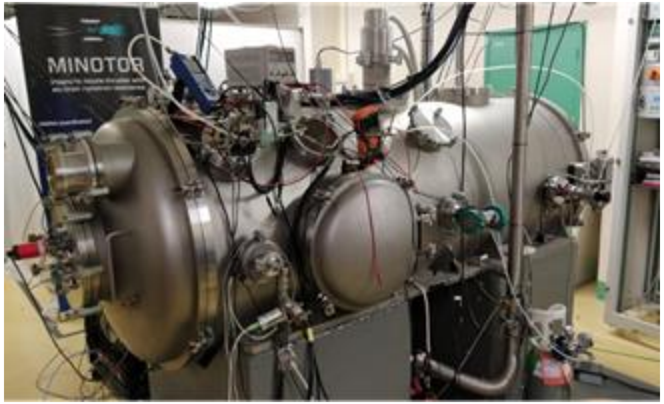

Vacuum chamber (ONERA)

The electron cyclotron resonance thruster ECRT, features a low temperature plasma discharge. Although the model cannot capture cyclotron damping, a cold-collisional model may suffice to provide reasonable damping.

Plasma thrusters decimate mission cost of space missions

This ECRT:
Dimensions: few cm
Flow rate: 0.1 mg/s
Thrust: ~1N
Thrust efficiency ~10/15%

ECRT prototype (ONERA)

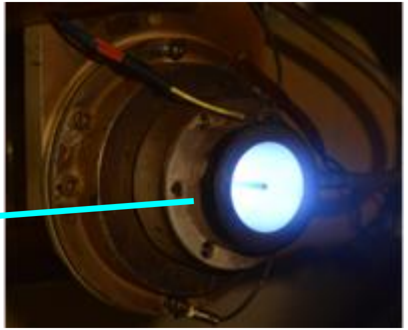

Magnetic nozzle

A scenario where the cold plasma model may suffice

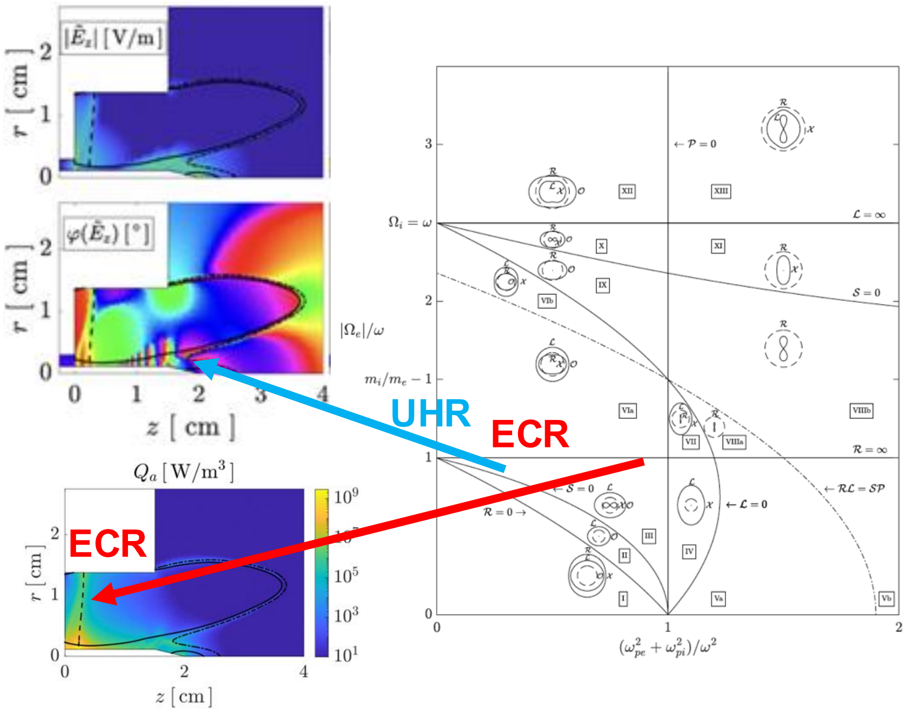

Studies show that parametric bounding surfaces affecting wave propagation in cold plasmas suffice to explain the thruster heating mechanism.

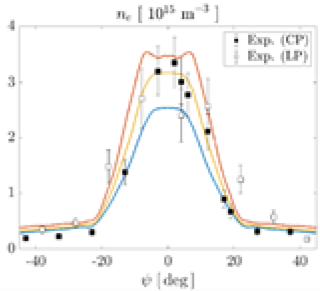

Validation and verification campaign of the thruster against experiments shows models strengths and weaknesses

Sources: Sanchez-Villar et al. PSST (2021)
Sanchez-Villar et al. PSST (2023)

Plasmas in tokamaks are further complex to model

- Kinetic approximation (e.g. hot plasma)
- Vlasov, unperturbed orbit and then applies a 1st order perturbation to the distribution function.
- The result is a set of integrals (expressions involving Bessel function and plasma dispersion function. For further information see Stix).

$$\boldsymbol{\chi}_s(\omega) = \left[\hat{z}\,\hat{z}\,\frac{2\,\omega_{ps}^2}{\omega\,k_\parallel\,v_{th}^2}\,\langle v_\parallel\rangle + \frac{\omega_{ps}^2}{\omega}\sum_{n=-\infty}^{+\infty} e^{-\lambda}\,Y_n(\lambda) \right]_s, \qquad \boldsymbol{\varepsilon}_s = \mathbf{I} + \boldsymbol{\chi}_s$$

$$Y_n(\lambda) = \begin{pmatrix} \frac{n^2}{\lambda} I_n(\lambda)\,A_n & -i\,n[I_n(\lambda) - I_n'(\lambda)]\,A_n & \frac{k_\perp}{\omega_{cs}}\frac{n}{\lambda} I_n(\lambda)\,B_n \\ i\,n[I_n(\lambda) - I_n'(\lambda)]\,A_n & \left(\frac{n^2}{\lambda} I_n(\lambda) + 2\lambda\,I_n'(\lambda) - 2\lambda\,I_n'(\lambda)\right) A_n & i\,\frac{k_\perp}{\omega_{cs}}[I_n(\lambda) - I_n'(\lambda)]\,B_n \\ \frac{k_\perp}{\omega_{cs}}\frac{n}{\lambda} I_n(\lambda)\,B_n & -i\,\frac{k_\parallel}{\omega_{cs}}[I_n(\lambda) - I_n'(\lambda)]\,B_n & \frac{2(\omega - n\,\omega_{cs})}{k_\parallel^2\,v_{th}^2} I_n(\lambda)\,B_n \end{pmatrix},$$

$$A_n = \frac{1}{k_\parallel\,v_{th}}\,Z_0(\zeta_n), \qquad B_n = \frac{1}{k_\parallel}\,[1 + \zeta_n\,Z_0(\zeta_n)],$$

$$Z_0(\zeta)\ \text{is the plasma dispersion function,} \qquad \zeta_n \equiv \frac{\omega - n\,\omega_{cs}}{k_\parallel\,v_{th}}, \qquad \lambda \equiv \frac{k_\perp^2\,v_{th}^2}{2\,\Omega_{cs}^2}.$$

- Important remarks
  - Non-local dielectric tensor which is a function of the distribution function, propagation direction $\boldsymbol{k}$, etc.
  - Includes as Finite Larmor radius effects ($k_\perp \rho$), Doppler ($k_\parallel v_\parallel$), Cyclotron damping ($n \neq 0$), and Landau Damping ($n = 0$).

Methods to solve Maxwell’s equations?

- Asymptotic methods ($\lambda \ll L$)
  - Used in weakly inhomogeneous plasmas in the small-wavelength limit ($\lambda \ll L$)
  - Geometrical Optics (GO)
  - Ray tracing or WKB approximation
  - Beam tracing or paraxial WKB approximation
  - Simplified solutions

- Full-wave methods ($\lambda \sim L$)
  - Solve Maxwell equations directly
  - Can deal with reflections
  - Different computational methods including finite differences (FD), finite elements (FE), or Spectral.
  - Computationally intensive

Multiple RF heating schemes are available

Scheme	Name	Typical f-band
ICRF/ICRH	Ion Cyclotron Range of Frequencies	25-120 MHz
ICRF-HHFW	High Harmonic Fast Wave	30-60 MHz
LHCD/LHH	Lower Hybrid	2-8 GHz
ECRH/ECCD	Electron Cyclotron Resonance	70-200 GHz
HH/HCD	Helicon	0.4 - 1 GHz
EBW (O-X-B/X-B)	Electron Bernstein Wave	2-30 GHz

Some examples of ICRF heating codes

- TORIC (Brambilla/Bilato)
  - Semi-spectral FEM model
  - Uses the FLR approximation
- AORSA (Jaeger)
  - Complete non-local, integral operator for the dielectric response
  - Valid to all orders in $k_\perp \rho$
  - Local cartesian grid
- Petra-M: multi-physics FEM platform implemented by S. Shiraiwa (PPPL)

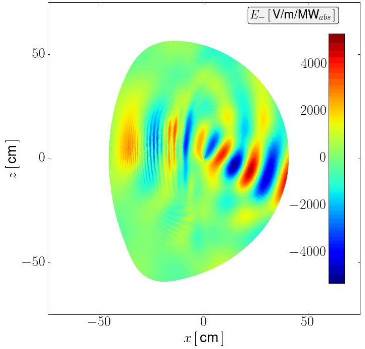

TORIC

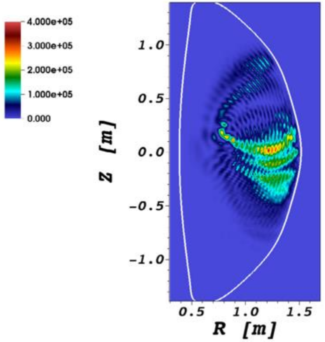

AORSA

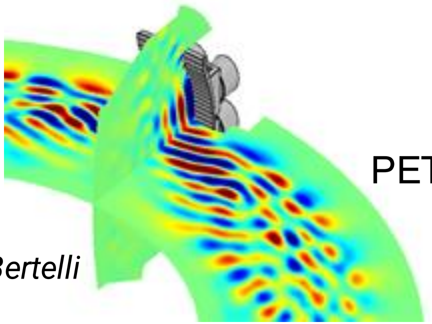

PETRA-M

Courtesy of S. Shiraiwa and N. Bertelli

ICRF heating schemes: Minority Ion Cyclotron (WEST)

- Fast magnetosonic wave (FW)
- 1-10% of hydrogen or helium-3 to Deut. plasmas
- FW polarization determined by majority ions
  - Strong coupling to minority at the fundamental ion cyclotron (IC) resonance $\omega = \omega_{cs}$
- Appearance of an ion-ion hybrid resonance (IIH)
  - Cut-off / resonance

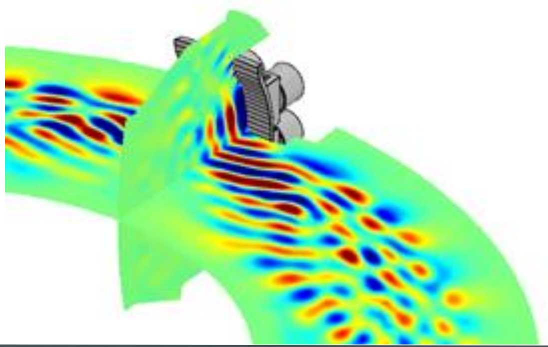

Mode conversion to a backward mode called the ion Bernstein wave (IBW). FW can still exist after the IIH. IBW absorbed by electrons via Landau damping. Conversion sensitive to minority concentration.

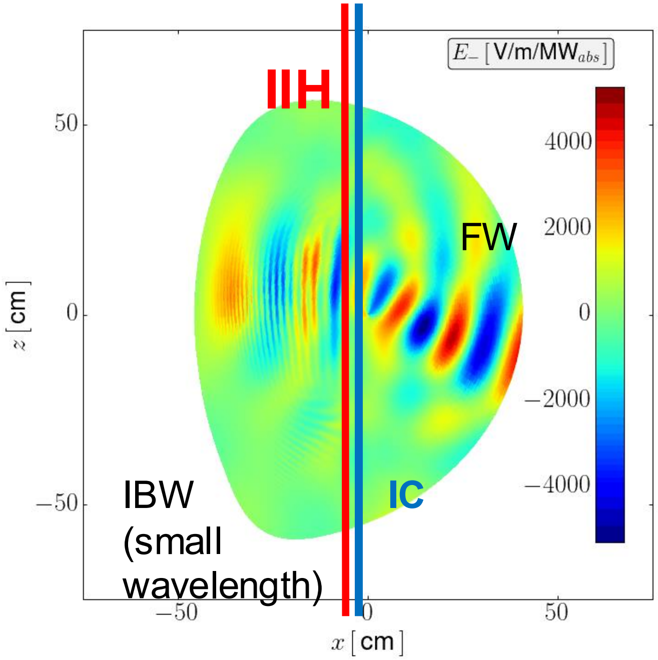

ICRF heating schemes: HHFW (NSTX-U)

- FW is the main propagating mode
- 12 strap antenna located at the outboard midplane.
- Absorption of ions (High-harmonic IC) and electrons via Landau damping.

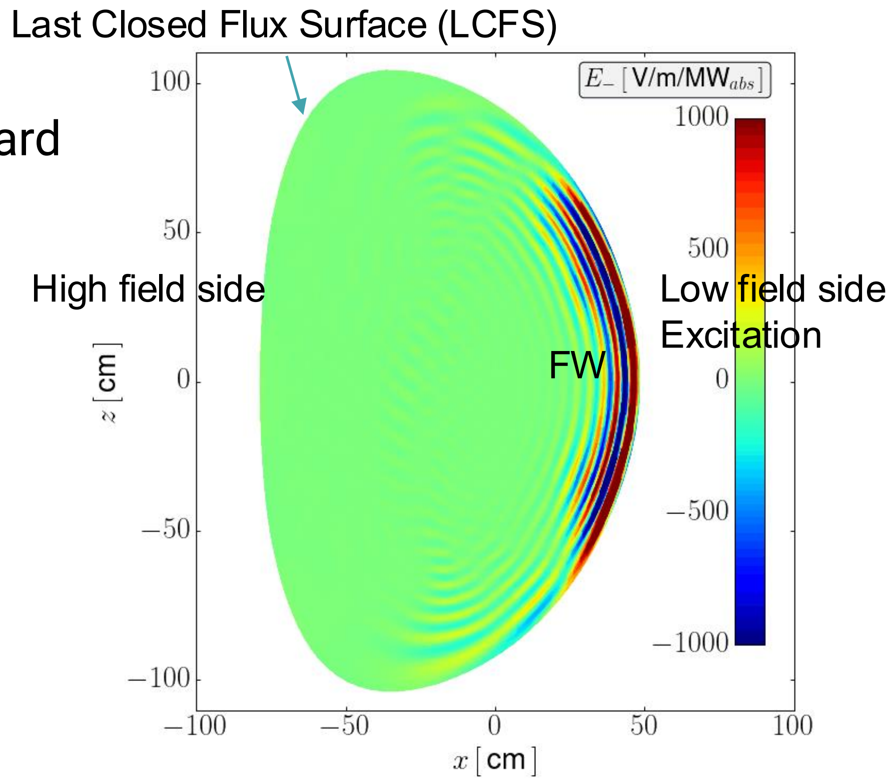

Simulation capability with different physics fidelity

Simulation capability with different physics fidelity

Physics Fidelity

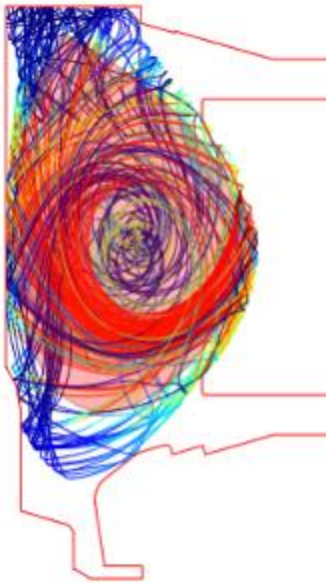

Computational Expenses

Simulation capability with different physics fidelity

Physics Fidelity

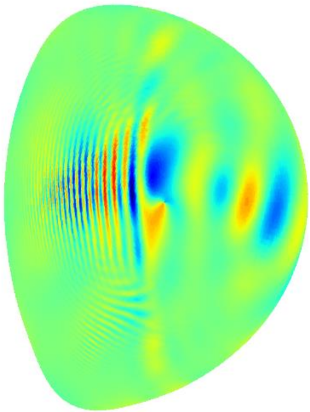

Computational Expenses

Simulation capability with different physics fidelity

Physics Fidelity

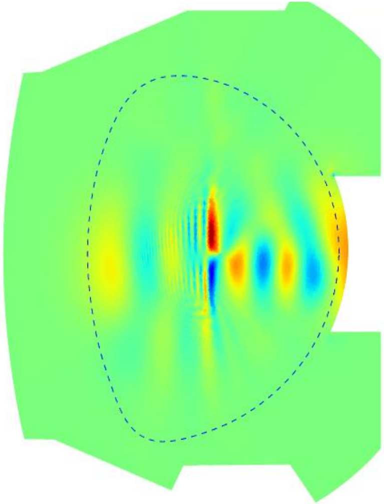

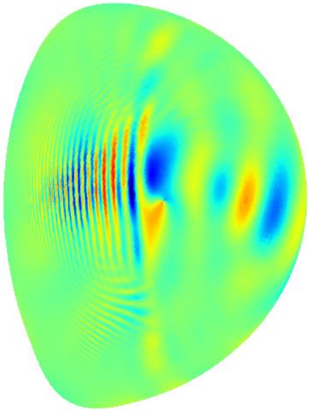

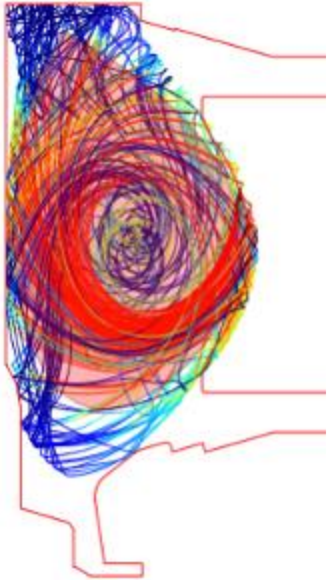

Computational Expenses

Simulation capability with different physics fidelity

Physics Fidelity

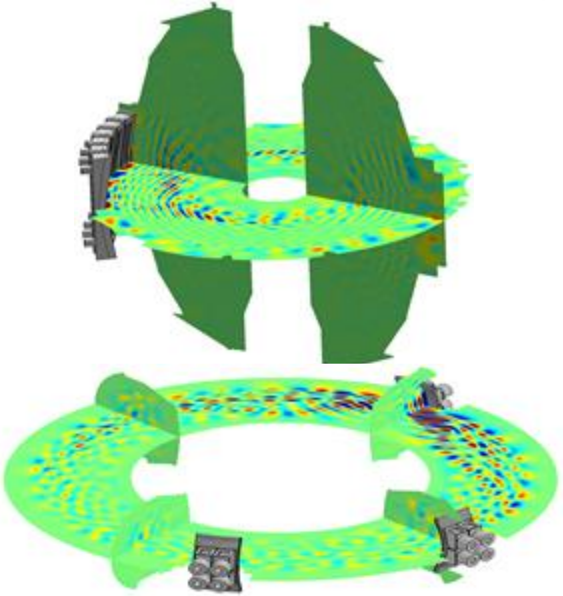

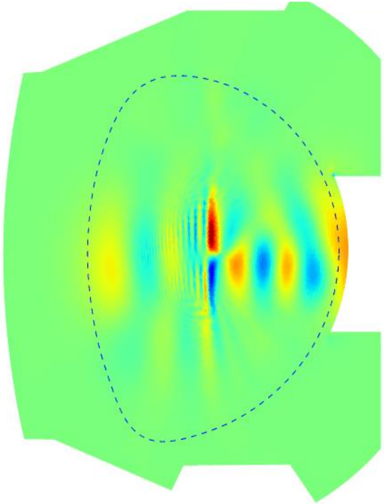

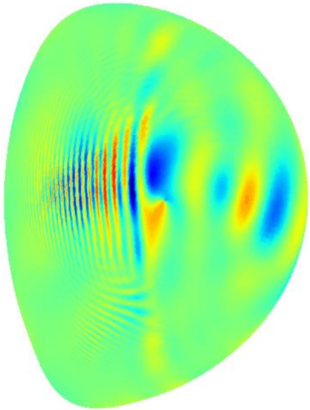

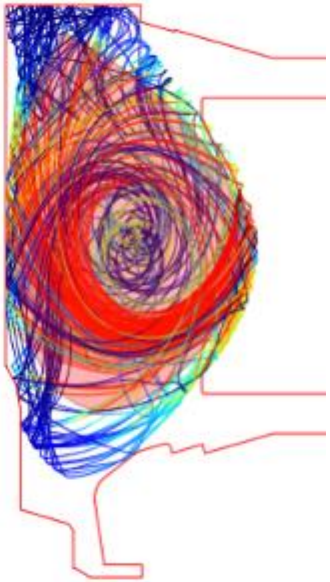

Computational Expenses

Heating profiles are critical outputs for integrated modeling

Physics Fidelity

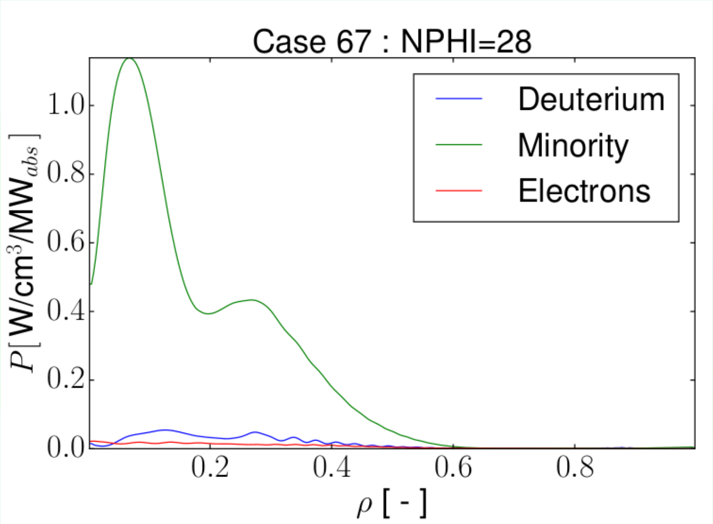

Computational Expenses

Artificial intelligence to accelerate predictions

Physics Fidelity

TORIC

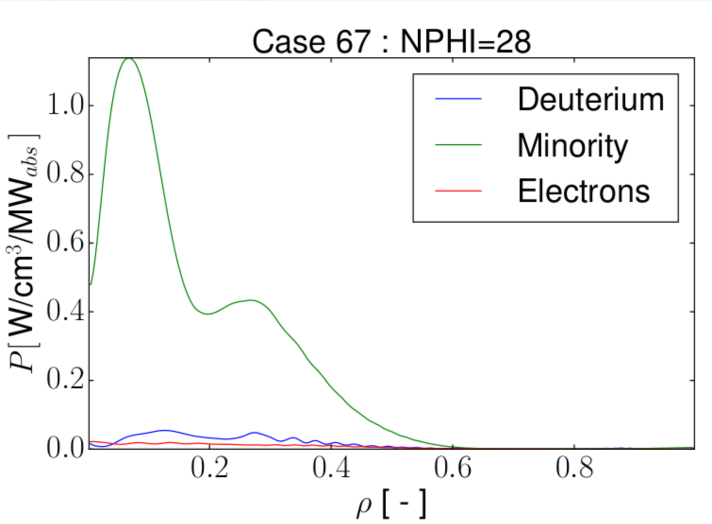

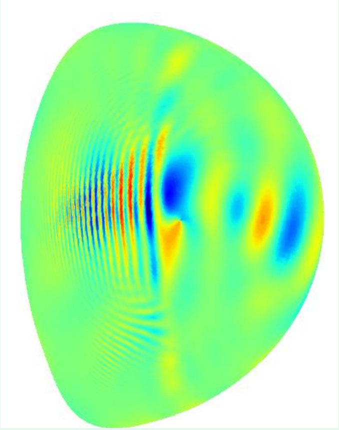

Simulation times unfeasible applications

- Scenario optimization
- Inter-shot predictive modeling
- Real-time control

Computational Expenses

Methodology

TORIC ICRF SPECTRUM SOLVER: O(min)

M. Brambilla (1999) PPCF ***41***
M. Brambilla (2002) PPCF ***44***

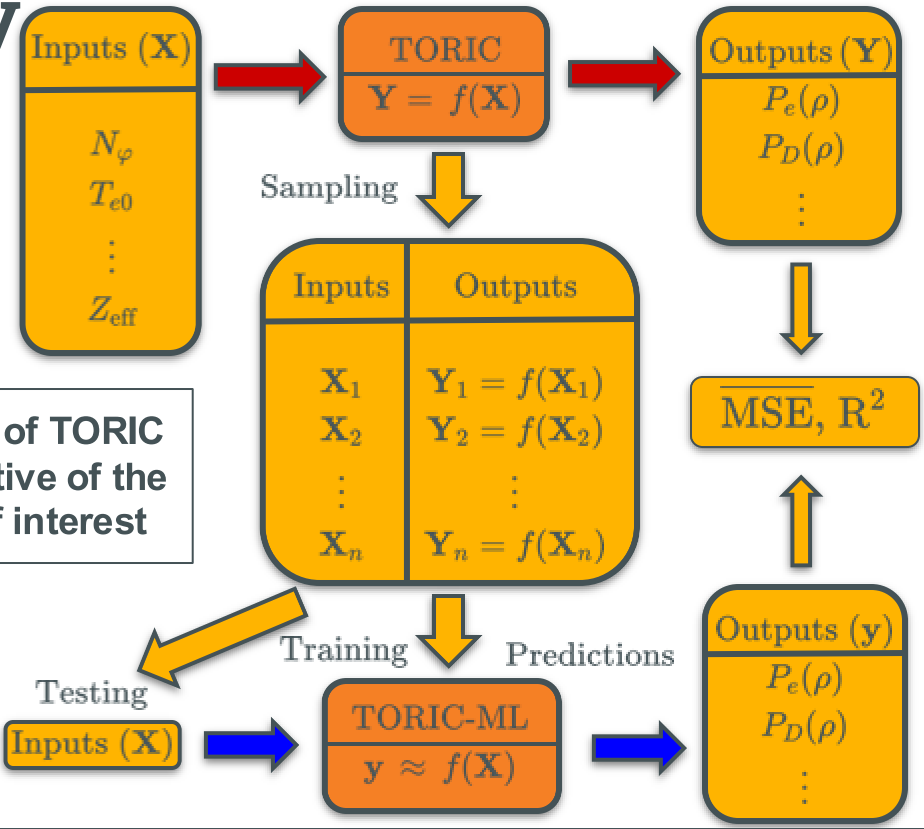

"Ground truths" are TORIC electron and ion power absorption 1D profiles

Generate a database of TORIC solutions representative of the parametric space of interest

Regression accuracy measured by:
1. Mean squared error (MSE)
2. Coefficient of determination(R2)

$$\text{MSE} = \frac{1}{N_y}\sum_{j=1}^{N_y}\frac{1}{N}\sum_{i=1}^{N}(y_{ij}-\hat{y}_{ij})^2\,,$$

$$\text{R}^2 = \frac{1}{N_y}\sum_{j=1}^{N_y}\left(1-\frac{\sum_{i=1}^{N}(y_{ij}-\hat{y}_{ij})^2}{\sum_{i=1}^{N}(y_{ij}-\bar{y}_j)^2}\right)$$

SURROGATE MODEL FOR THE FORWARD PROBLEM: O(μs)

Artificial intelligence and machine learning (AI/ML)

- Artificial Intelligence (AI):
  - Broad goal of creating system that can perform intelligent tasks

- Machine Learning (ML):
  - A subset of AI where algorithms learn patterns from data rather than follow explicit rules

- High-performance computing (HPC) be used to train and optimize the models and generate/manage the datasets

ML paradigms

Paradigms	General Goal	Examples of Algorithms
Supervised	Learn inputs->Outputs mapping	Linear, Random Forest, Gaussian Processes, Neural Networks
Unsupervised	Discover hidden structure	k-means, DBSCAN
Reinforcement	Learn to make sequences of decisions	Q-learning, Policy Gradients

Supervised AI/ML models for Regression

- Random Forest Regressor (RFR)
  - Ensemble of decision trees
  - Final prediction average of the trees
  - By splitting feature values to maximize information gain at each node, RFR can deal with nonlinear relationships
  - Available in **scikit-learn**

- Multilayer perceptron (MLP)
  - Feed-forward neural network built of perceptrons that together can approximate highly nonlinear mappings
  - Careful hyperparameter tuning required
  - Bayesian optimization. **PyTorch** Recommended

- Gaussian Process Regressor (GPR):
  - Bayesian regression method that treats predictions as distributions
  - Provides uncertainty quantification
  - Implementation with **TensorFlow** and **GPflow**

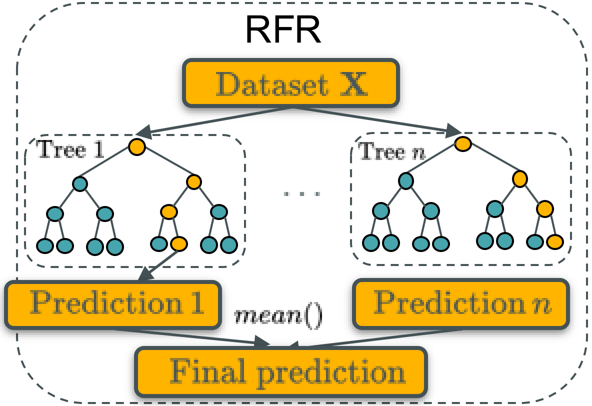

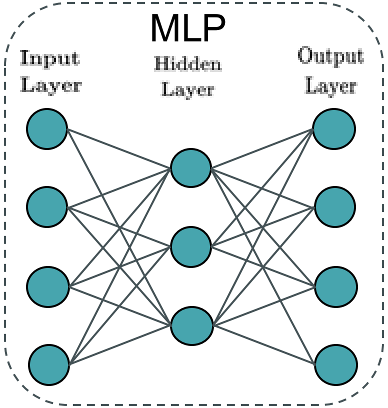

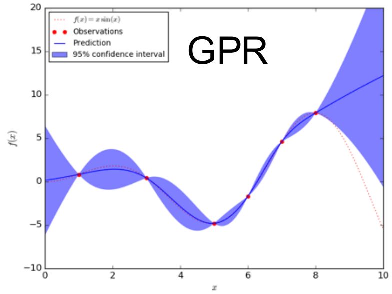

Two databases for flat-top operation of NSTX and WEST

- Heating schemes:
  - HHFW: $\omega > \Omega_{ci}$
  - IC minority: $\omega \sim \Omega_{ci}$
- Plasma species: D (D-H).
- Equilibriums are assumed to be fixed to:

- **Flat-top** scenario plasma properties (e.g. temperature, density, etc) as :

$$T_e = (T_{e0} - T_{e1})(1 - \rho^{\alpha})^{\beta} + T_{e1}$$

  - 0/1 -> core/edge
  - α and β : profile shape exponents

G. Taylor et al. (2012) PoP ***19***
J. Bucalossi et al. (2022) NF ***62***

NSTX - Shot 138506

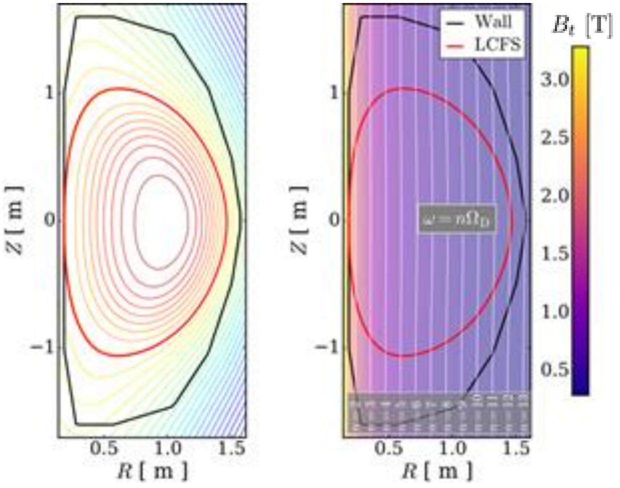

WEST - Shot 56898

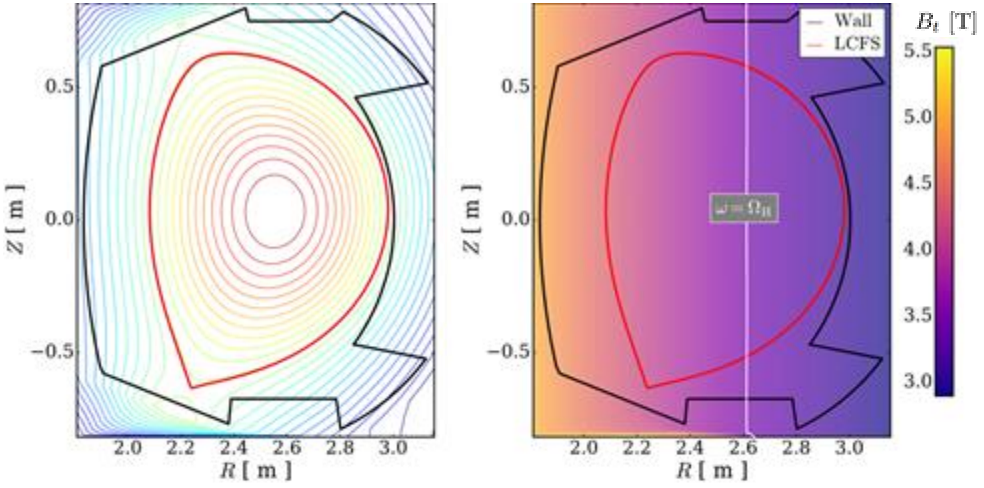

Data is standardized and then analyzed and refined

- **Standardization** of data using training data, and **principal component analysis** on WEST outputs → dimensionality reduction, improved profile inference time and accuracy.
- Exploratory analysis resulted in outlier identification in the NSTX database:

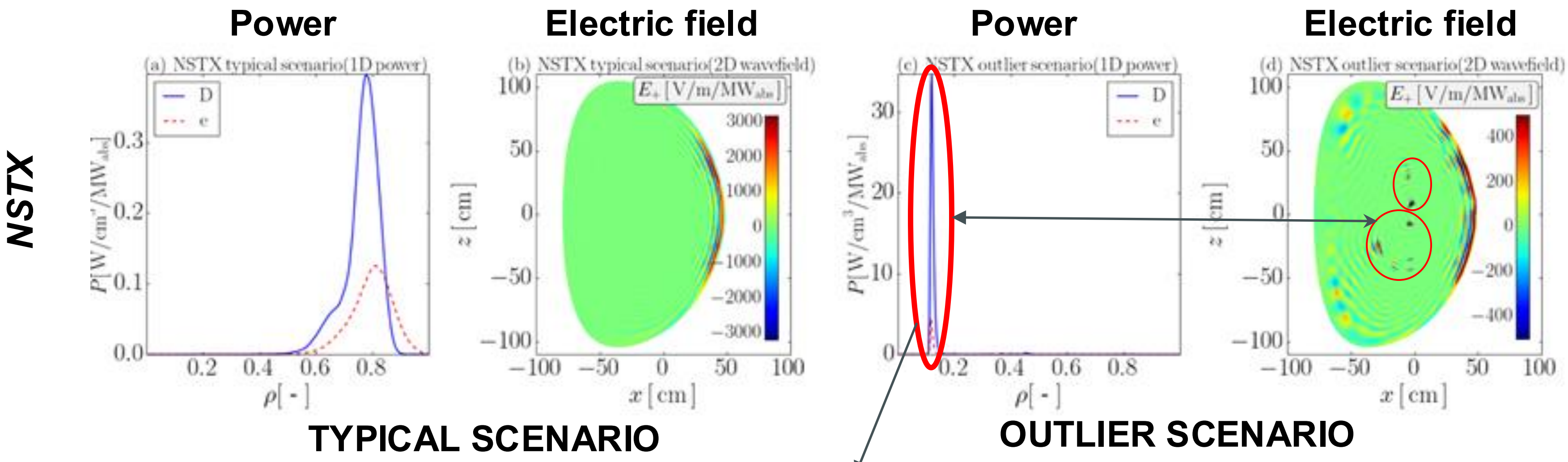

22% outliers understood to be numerical.

Full-wave + ML enables robust real-time capable ICRF models

- **FAST:** Inference time ⇨ TORIC O(min) | TORIC-ML **O(μs)**
- **ACCURATE:** Regression accuracy ⇨ **NSTX R^2= 0.95** ; WEST **R^2= 0.7**

Deuterium - NSTX

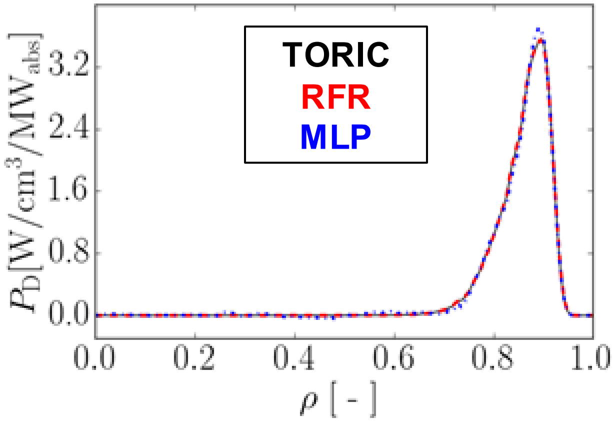

Hydrogen - WEST

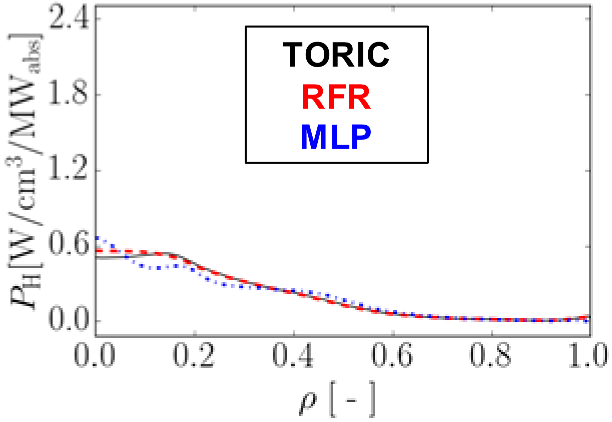

Full-wave + ML enables robust real-time capable ICRF models

- **FAST:** Inference time ⇨ TORIC O(min) | TORIC-ML **O(μs)**
- **ACCURATE:** Regression accuracy ⇨ **NSTX R^2= 0.95** ; WEST **R^2= 0.7**
- **ROBUST:** Predict physical profiles beyond the original model capability, overcoming numerically challenging scenarios in HHFW

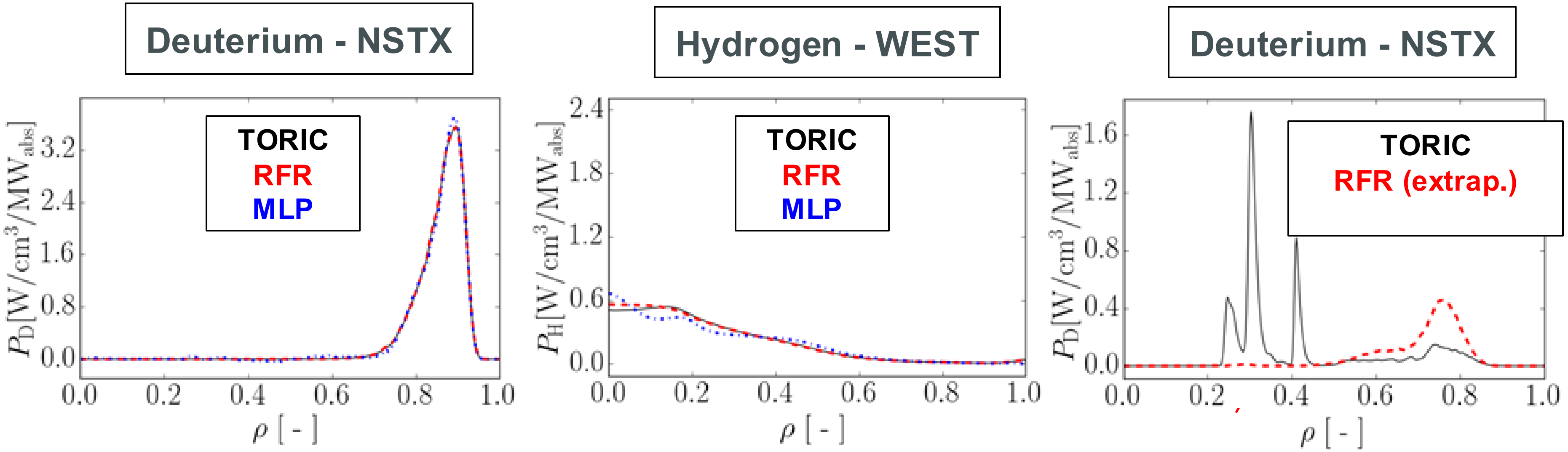

Full-wave + ML enables robust real-time capable ICRF models

- **FAST:** Inference time ⇨ TORIC O(min) | TORIC-ML **O(μs)**
- **ACCURATE:** Regression accuracy ⇨ **NSTX R^2= 0.95** ; WEST **R^2= 0.7**
- **ROBUST:** Predict physical profiles beyond the original model capability, overcoming numerically challenging scenarios in HHFW

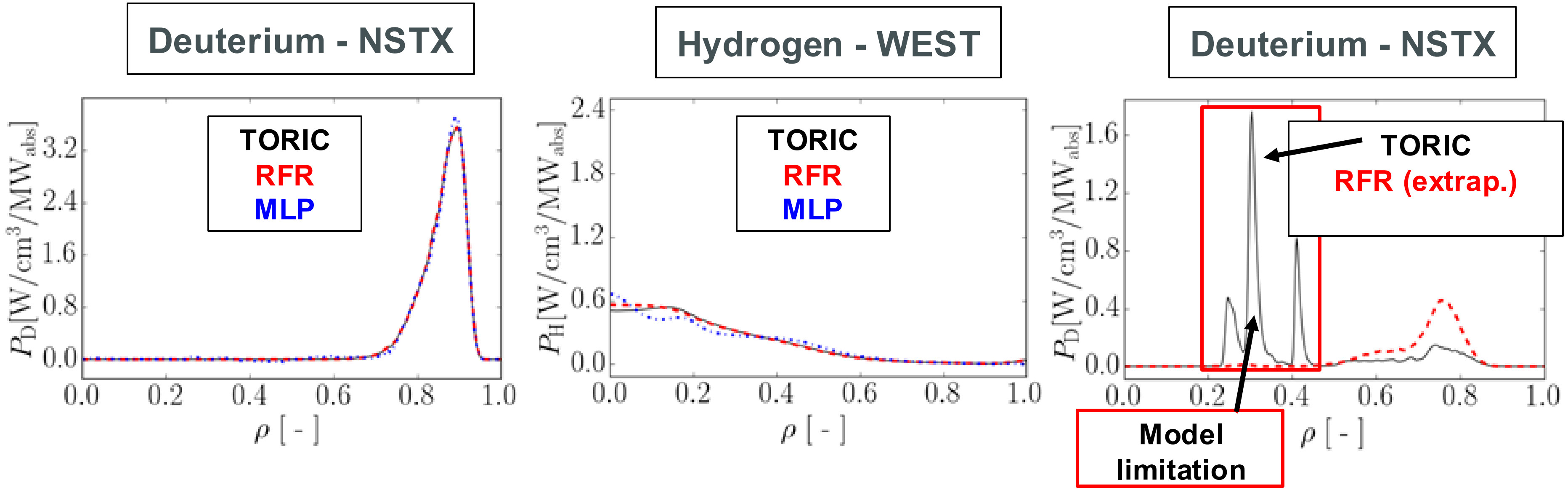

Full-wave + ML enables robust real-time capable ICRF models

- **FAST:** Inference time ⇨ TORIC O(min) | TORIC-ML O(μs)
- **ACCURATE:** Regression accuracy ⇨ NSTX R^2= 0.95 ; WEST R^2= 0.7
- **ROBUST:** Predict physical profiles beyond the original model capability, overcoming numerically challenging scenarios in HHFW

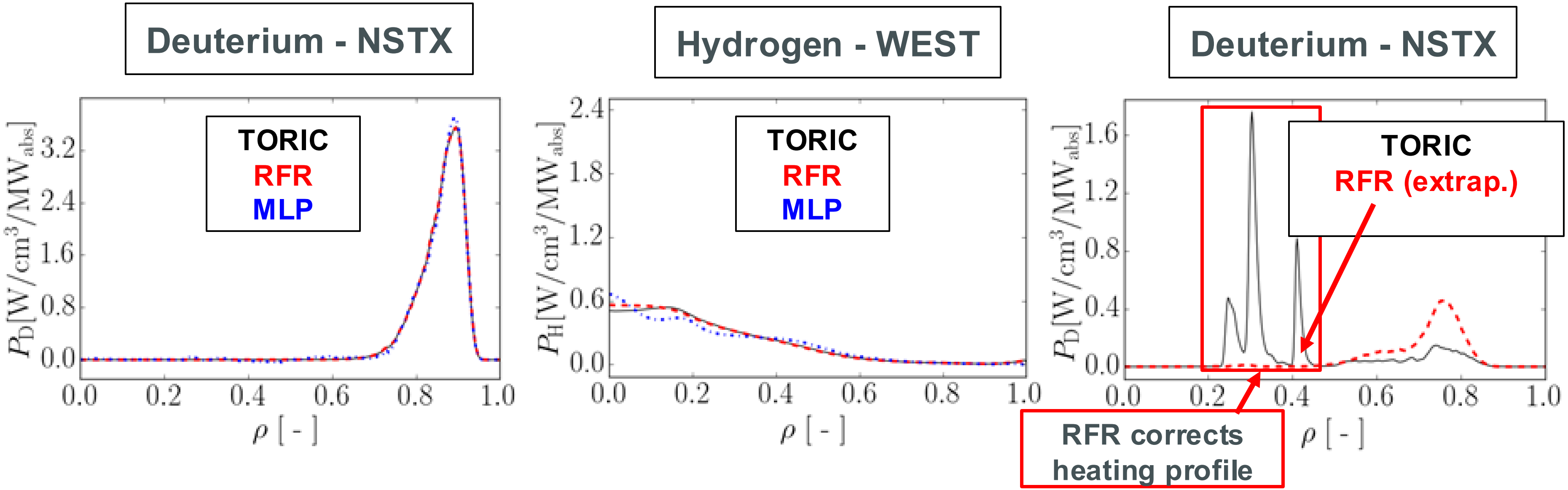

Full-wave + ML enables robust real-time capable ICRF models

- **FAST:** Inference time ⇨ TORIC O(min) | TORIC-ML O(μs)
- **ACCURATE:** Regression accuracy ⇨ NSTX R^2= 0.95 ; WEST R^2= 0.7
- **ROBUST:** Predict physical profiles beyond the original model capability, overcoming numerically challenging scenarios in HHFW

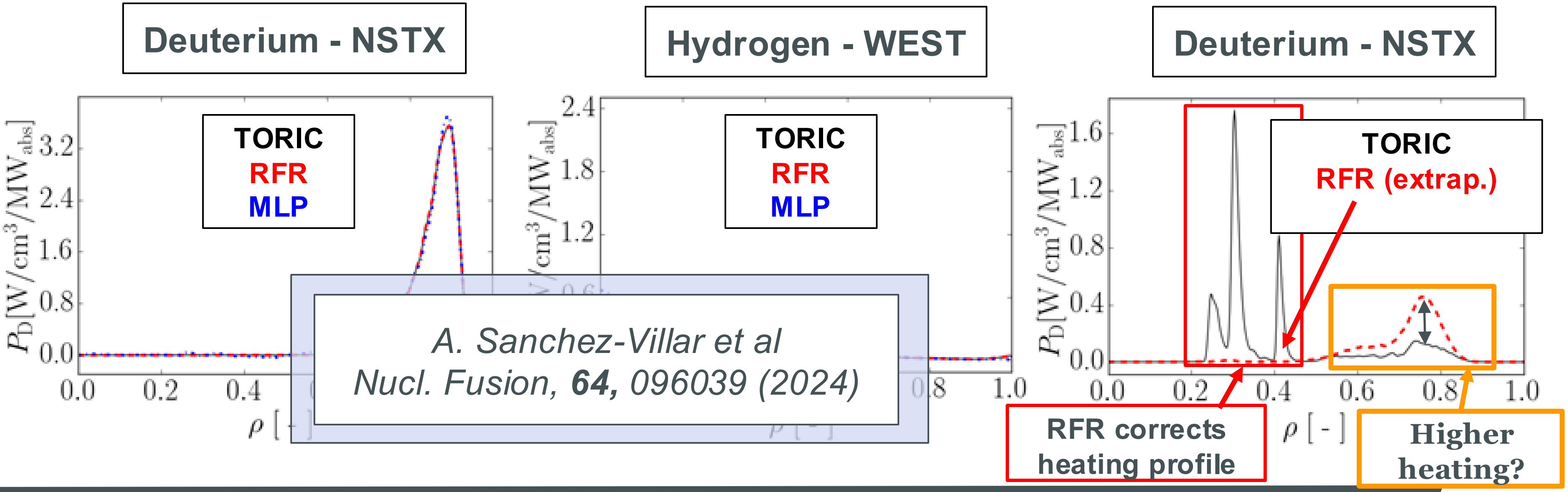

A. Sanchez-Villar et al
*Nucl. Fusion, **64**, 096039 (2024)*

Full-wave + ML enables robust real-time capable ICRF models

- **FAST:** Inference time ⇨ TORIC O(min) | TORIC-ML **O(μs)**
- **ACCURATE:** Regression accuracy ⇨ **NSTX R^2= 0.95** ; WEST **R^2= 0.7**
- **ROBUST:** Predict physical profiles beyond the original model capability, overcoming numerically challenging scenarios in HHFW

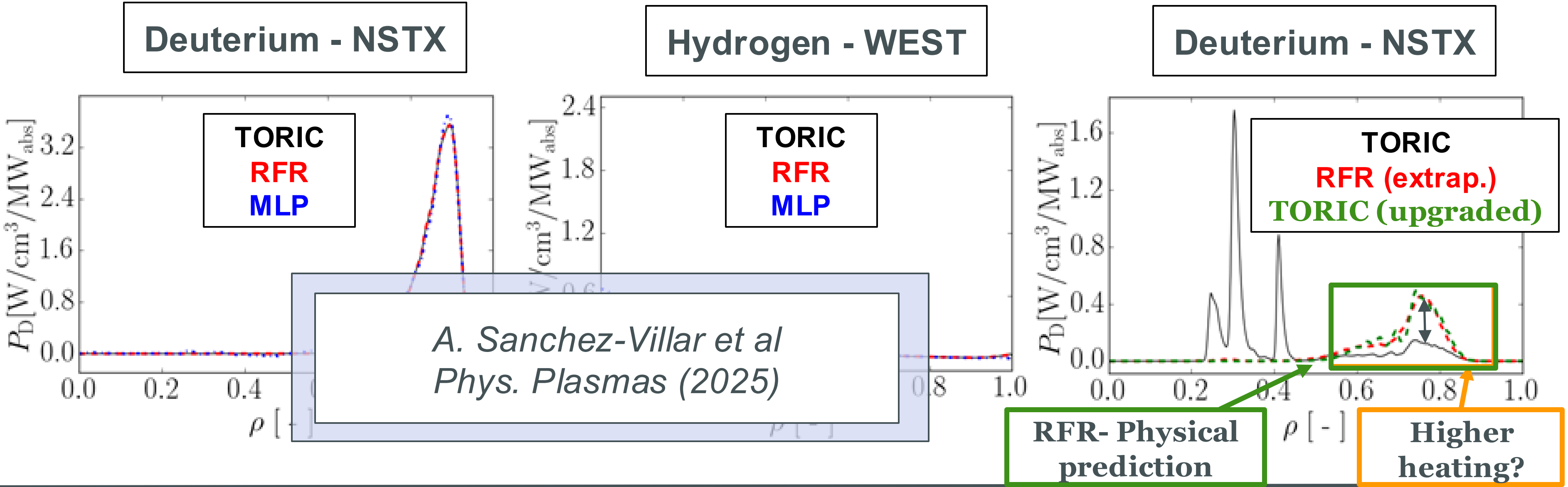

A. Sanchez-Villar et al
Phys. Plasmas (2025)

Comparison at extrapolated inference to HHFW outliers

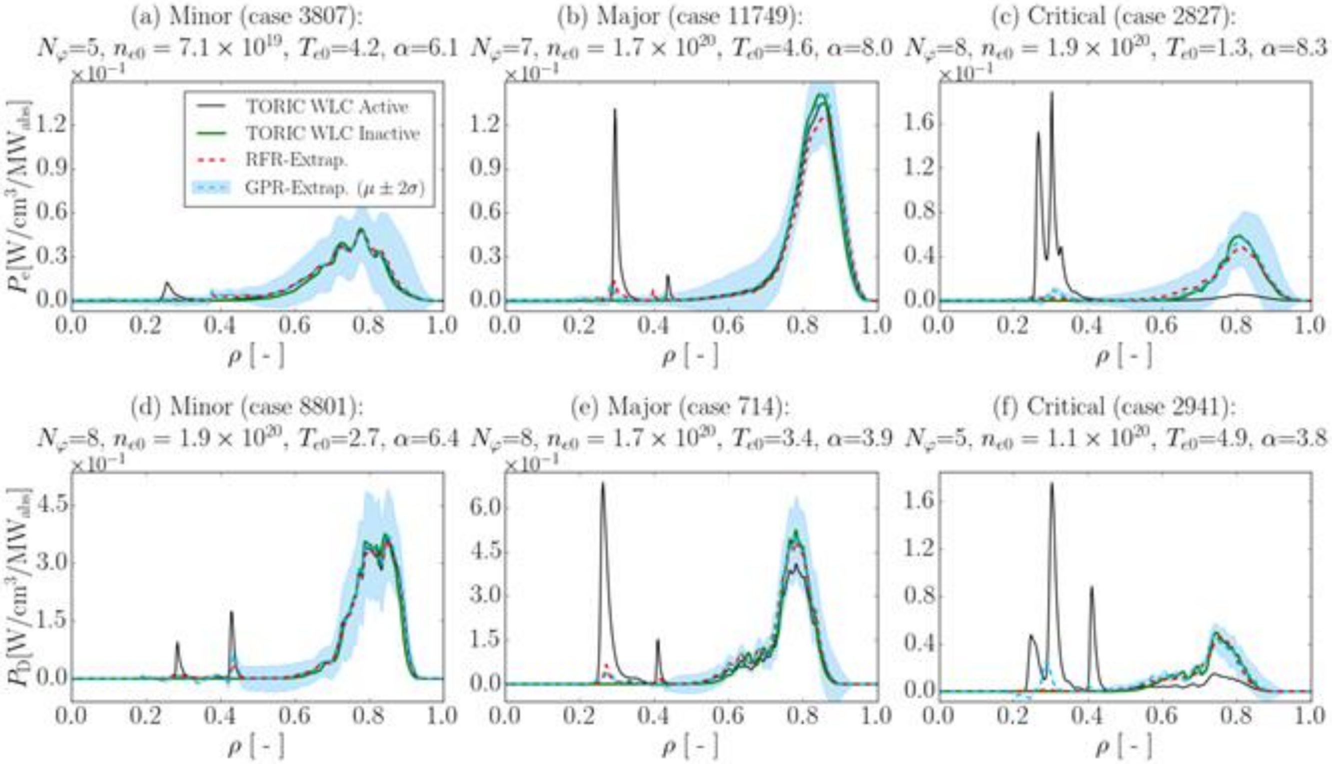

*Á. Sánchez-Villar et al
Phys. Plasmas (2025)*

Final models for HHFW at NSTX (including GPR)

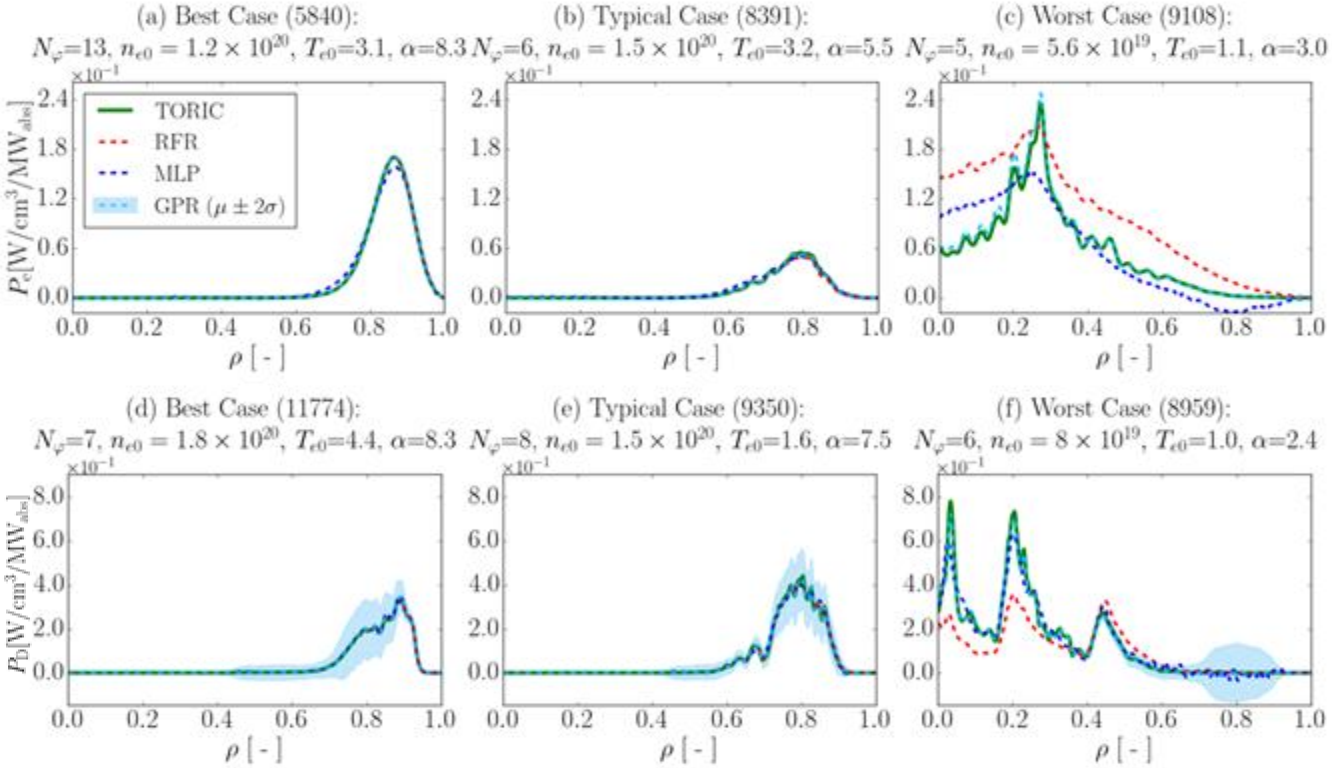

Á. Sánchez-Villar et al Phys. Plasmas (2025)

Bayesian Optimization Methods used to develop an Automated Surrogate Model Generator Suite

- Train, test, save, load surrogates & results.
- Automatically optimize the hyperparameters (including architecture) for the RFR, MLP and GPR models for a given dataset + final training.

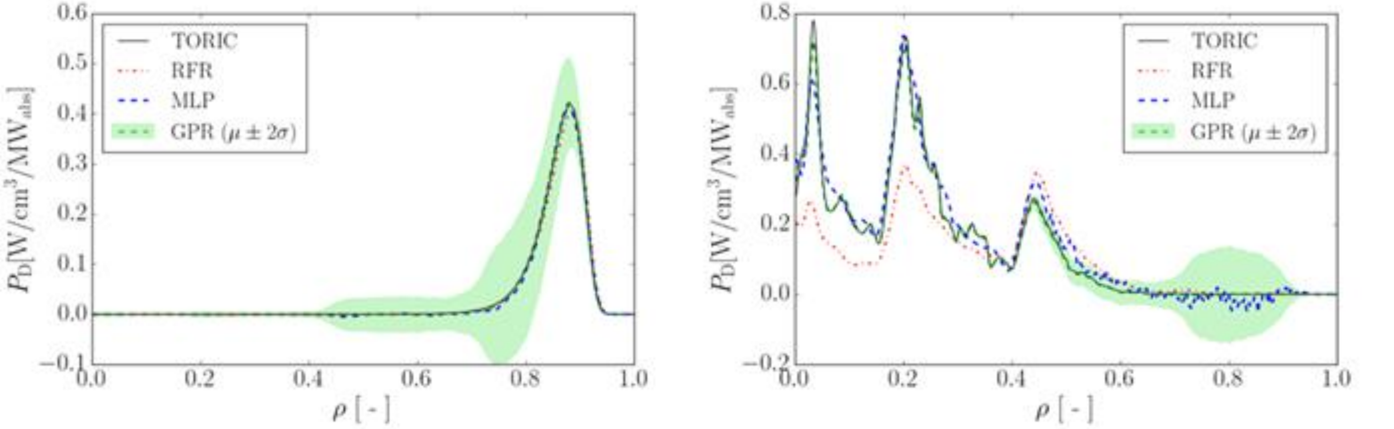

(a) Single-pass absorption (b) Multi-pass absorption

Figure 1: Machine learning based deuterium power absorption predictions from the RFR (red dash-dotted), MLP (blue dashed), and GPR (green) models obtained with the Automated Surrogate Model Generator Suite are shown in (a) strong single-pass and (b) multi-pass absorption scenarios in NSTX, and compared to the reference computational model TORIC (black solid). For the GPR we show the mean prediction (μ, green dashed) and the 95% confidence interval based on the estimated standard deviation (σ, green shadow).

Some final references

Email: asvillar@pppl.gov | asvillar@princeton.edu

Books RF:
Stix, Brambilla, Dawson, Bittencourt

Books AI/ML:
Bishop,
Goodfellow, etc.

RF models:
TORIC, AORSA,
Petra-M, etc.

ML models:
PyTorch, TensorFlow,
Sklearn, Gpflow,
BoTorch

Some links:

- www.github.com/piScope/piScope
- www.github.com/piScope/PetraM_RF
- www.scikit-learn.org
- www.pytorch.org ; www.tensorflow.org

Special thanks: to N. Bertelli, S. Shiraiwa, and to the organizers and participants of the SULI